4806 *Chem. Mater.* **2010,** *22,* 4806–4813
DOI:10.1021/cm101412d

CHEMISTRY OF MATERIALS
Article

Fabrication of a Vertically Aligned Ferroelectric Perovskite Nanowire Array on Conducting Substrate

Badro Im,[†] Hwichan Jun,[†] Kyung Hee Lee,[†] Sung-Ho Lee,[‡] Il Kyu Yang,[‡] Yoon Hee Jeong,[‡] and Jae Sung Lee*,[†]

[†]*Department of Chemical Engineering and* [‡]*Department of Physics, Pohang University of Science and Technology* (*POSTECH*), *San 31, Hyoja-dong, Nam-gu, Pohang, Kyungbuk, 790-784, South Korea*

Received May 20, 2010. Revised Manuscript Received June 30, 2010

A new fabrication process of a vertically aligned ferroelectric perovskite $PbTiO_3$ nanowire array on Ti substrate is presented. Polycrystalline TiO_2 nanotubes are first fabricated by anodic oxidation of Ti foil and then treated hydrothermally in a lead acetate solution to obtain single-crystalline nanowires. This nanotube-to-nanowire transformation on conducting substrate could be described by a swelling-and-rupture mechanism, in which individually well-developed nanotubes are swollen and broken along the friction planes because of difference in the directions of expansion force. Nanowires with a uniform diameter of ca. 40 nm and a length of 10 μm show single-crystalline nature over the entire length of nanowires and ultrahigh density corresponding to ca. 0.22 Tb inch^{-2}. The ferroelectric property of individual $PbTiO_3$ nanowires and whole area of nanowire arrays has been demonstrated by piezo-response force microscopy.

1. Introduction

One-dimensional (1-D) ferroelectric nanomaterials on substrates are of great interest because of their peculiar physical properties of large surface area, excellent charge transport, and outstanding ferroelectric properties.[1,2] Especially, well-aligned ferroelectric nanowire arrays on a conducting substrate are suitable for three-dimensional device elements in miniaturized ferroelectric devices. They also provide an opportunity to study the size and morphology dependence of optical, magnetic, and electronic properties. For example, there is a size limit, known as the superparaelectric limit, below which ferroelectricity vanishes. Yet a fabrication technique for such ferroelectric nanowire arrays has not been well established. Most important ferroelectric materials are oxides with a perovskite structure such as $PbTiO_3$, $BaTiO_3$, and $Pb(Zr,Ti)O_3$ because this flexible structure can accommodate a wide variety of atoms characterized by a perovskite tolerance factor.[3] These ferroelectric perovskite materials exhibit a spontaneous polarization below the Curie temperature which can be reversed by an electric field. They also have large nonlinear optical coefficients and large dielectric constants. These properties are exploited in applications such as nonvolatile memory devices, thermistors, multilayer capacitors, and dynamic random access memories.[4]

The perovskite oxides are synthesized by a number of routes.[5] Yet, comparatively little work has been done on the fabrication of ternary perovskite oxide nanowires or tubes on a conducting substrate, a basic unit of miniaturized ferroelectric devices. A technique to prepare perovskite nanotubes/nanowires is the sol−gel template method, which uses nanoporous silicon or alumina as a hard template.[6−9] Thus, the pores of the template are filled up with a suitable precursor solution and annealed to form perovskite oxides. The perovskite material could be separated from the template by etching the template away. The process is rather complicated, and it is difficult to obtain uniform products because filling the small pores is not easy. The other method is based on electrochemical anodization, a highly reproducible and powerful technique to synthesize many kinds of 1-D nanotubes. Thus, anodic TiO_2 nanotubes are synthesized first on Ti foil and undergo hydrothermal reactions in metal precursor solutions to produce ferroelectric perovskite nanotubes of $PbTiO_3$, $BaTiO_3$, and $Pb(Zr,Ti)O_3$.[10−14] From this

*Corresponding author. Tel: 82-54-279-2266. Fax: 82-54-279-5528. E-mail: jlee@postech.ac.kr.

(1) Kim, J.; Yang, S. A.; Choi, Y. C.; Han, J. K.; Jeong, K. O.; Yun, Y. J.; Kim, D. J.; Yang, S. M.; Yoon, D.; Cheong, H.; Chang, K. S.; Noh, T. W.; Bu, S. D. *Nano Lett.* **2008**, *8*(7), 1813.
(2) Law, M.; Greene, L. E.; Johnson, J. C.; Saykally, R.; Yang, P. *Nature* **2005**, *4*, 455.
(3) Joshi, U. A.; Lee, J. S. *Small* **2005**, *1*, 1172.
(4) Feng, X.; Shankar, K.; Varghese, O. K.; Paulose, M.; Latempa, T. J.; Grimes, C. A. *Nano Lett.* **2008**, *8*(11), 3781.
(5) Zhu, X *Recent Pat. Nanotechnol.* **2009**, *3*, 42.
(6) Mao, Y. B.; Parka, T. J.; Wong, S. S. *Chem Commun.* **2005**, 5721.
(7) Hernandez, B. A.; Chang, K. S.; Fisher, E. R.; Dohaut, P. K. *Chem. Mater.* **2002**, *14*, 480.
(8) Zhang, X. Y.; Zhao, X.; Lai, C. W.; Wang, J.; Tang, X. G.; Dai, J. Y. *Appl. Phys. Lett.* **2004**, *85*, 4190.
(9) Hsu, M. C.; Leu, I. C.; Sun, Y. M.; Hon, M. H. *J. Solid State Chem.* **2006**, *179*, 1421.
(10) Liu, L.; Ning, T.; Ren, Y.; Sun, Z.; Wang, F.; Zhou, W.; Xie, S.; Song, L.; Luo, S.; Liu, D.; Shen, J.; Ma, W.; Zhou, Y. *Mater. Sci. Eng. B.* **2008**, *149*, 41.
(11) Padture, N. P.; Wei, X. *J. Am. Ceram. Soc.* **2003**, *86*(12), 2215.
(12) Wei, X.; Vasiliev, A. L.; Padture, N. P. *J. Mater. Res.* **2005**, *20*(8), 2140.
(13) Yang, Y.; Wang, X.; Zhong, C.; Sun, C.; Yao, G.; Li, L. *J. Am. Ceram. Soc.* **2008**, *91*(10), 3388.
(14) Yang, Y.; Wang, X.; Zhong, C.; Sun, C.; Li, L. *Appl. Phys. Lett.* **2008**, *92*, 122907.

Published on Web 07/26/2010
© 2010 American Chemical Society

technique, the formation of only nanotubes have been reported, which are usually of particle-stacked, polycrystalline structure, and therefore, it is difficult to expect unique characteristics originating from the crystalline 1-D structure.

Here, we report, for the first time, a convenient fabrication method of vertically aligned $PbTiO_3$ nanowire arrays of high aspect ratio grown on Ti substrate by hydrothermal treatment of anodic titanate nanotubes. As mentioned, the transformation of TiO_2 nanotubes into $PbTiO_3$ by the hydrothermal method was reported, but product morphology was nanotubes of polycrystalline nature.[14] In contrast, our method produces nanowire arrays made of single crystal $PbTiO_3$. We also demonstrate that this $PbTiO_3$ nanowire arrays have ferroelectric properties. The nanowires are 40 nm in diameter and 10 μm in length, and the array has the ultrahigh density corresponding to ca. 0.22 Tb inch^{-2} of ferroelectric memory.

2. Experimental Section

2.1. Anodic Oxidation of Ti Foil. First step of the fabrication is anodic oxidation of Ti foil in oxide-soluble solution to obtain well-developed titania nanotubes. Titania nanotubes were grown from a pure titanium foil (99.7%, 250 μm thick, Aldrich) with a size of 1.5 cm $\times$ 1.5 cm, cleaned by sonication in acetone, isopropyl alcohol, and ethanol and dried under N_2 atmosphere. Copper wire was attached to Ti foil using silver paste, and all borders and edges were shielded by nonconductive epoxy. The potentiostatic anodization process was performed in a two-electrode electrochemical cell equipped with Ti foil (anode) and platinum mesh (cathode). The distance of two-electrodes was 3 cm. The TiO_2 nanotubes were fabricated on cleaned Ti foil by anodization at 60 V for 30 min at 30 °C in a solution of 0.3 wt % NH_4F and 2 vol% deionized water dissolved in ethylene glycol.[15] The as-anodized sample was rinsed with ethylene glycol and deionized water. Epoxy-removed TiO_2 nanotube film on Ti substrate was annealed at 400 °C for 3 h to transform amorphorous titanate into anatase TiO_2 phase.

2.2. Hydrothermal Reaction. The second step is the hydrothermal reaction to convert the anatase TiO_2 into $PbTiO_3$. The hydrothermal treatment was carried out in a Teflon-vessel fitted into a stainless steel reactor containing 0.002 M Pb acetate trihydrate dissolved in 80 mL of CO_2-free water under N_2 atmosphere. The reactor was placed in a convection oven at 280 °C for 6 h without disruption. Finally, the product was rinsed with CO_2-free deionized water and dried in a vacuum oven. The Pb acetate concentration and temperature were important factors for high quality nanowire formation. We synthesized $PbTiO_3$ nanowires under 0.002−0.005 M Pb acetate concentration and 260−300 °C. The pure nanowires were not formed under Pb acetate concentration lower than 0.002 M or temperature below 260 °C. The best condition was 0.002 M and 280 °C.

2.3. Sample Characterization. Top-surface and cross-sectional images are analyzed by field emission scanning electron microscopy (FE-SEM, JEOL JSM-7401F and Philips XL30S FEG). The structure was observed by the field emission transmission electron microscopy images (FE-TEM, JEM-2100F). The crystalline phase of the sample was determined by X-ray diffraction (XRD, PANalytical X'Pert diffractometer with an X'Celerator detector, Cu Kα radiation) The measurements for extended X-ray absorption fine structure (EXAFS) were performed at the beamline 5A in the Pohang Accelerator Laboratory (PAL), Korea, to determine the structure and local atomic arrangements. X-ray photoelectron spectroscopy (XPS, VG Scientific, ESCALAB 220iXL) was used to analyze the surface compositions using a Mg Kα X-ray source (1253.6 eV) at room temperature.

2.4. Measurements of Ferroelectric Properties. PFM studies were carried out using a commercial atomic force microscope (AFM; XEI-100, PSIA). The Ti substrate served as a bottom electrode, and a conductive AFM tip (Si tip with Au coating on both sides, model FORTGG, APPNANO, USA) served as a top electrode. The tip radius was below 30 nm, frequency 62 kHz, and the spring constant 3 N m^{-1}. In order to detect the piezoreponse signal, a lock-in technique was used. As the AFM tip scanned, an AC voltage of 1 V at 17 kHz was applied. When a small AC voltage at a certain frequency was applied to the piezoelectric material, the material vibrated with the same frequency due to the converse piezorelectric effect. This vibration was detected by the AFM tip, and the lock-in amplifier decoupled the signals into an amplitude of piezoreponse and phase information. After imaging, a piezoelectric d33 was measured. The AFM tip was fixed at the desired position, and the amplitude and phase of vertical vibration were measured with AC voltage and continuously varying the DC bias voltage from −10 to 10 V. If a material is ferroelectric, a hysteresis loop appears.

3. Results and Discussion

3.1. Fabrication of $PbTiO_3$ Nanowires on Ti Substrate from Swelling and Rupture of TiO_2 Nanotubes. Anodic oxidation of Ti foil in a solution of 0.3 wt % NH_4F and 2 vol % deionized water dissolved in ethylene glycol produced well-developed titania nanotubes grown from 1.5 cm $\times$ 1.5 cm titanium foil. The condition has been optimized to yield a high quality nanotube array with excellent regularity. Figure 1a,b shows top-surface and cross-sectional images of field emission scanning electron microscopy for anodized TiO_2 nanotubes after annealing at 400 °C. Uniform and densely packed nanotube arrays of high quality are evident with an average tube diameter of 120 nm, a wall thickness of 20 nm, and a length of about 10 μm. The nanotubes are individually well-developed in shape with obvious spacing between them, and some of them form bundles. Both as-anodized titanate (amorphous) and annealed TiO_2 (anatase) showed the same tube morphology despite the phase change. The detailed structure of a TiO_2 nanotube was investigated by FE-TEM. As shown in Figure 1c,d, randomly distributed patches of lattice fringes indicate that the tube wall of TiO_2 is made of particle-stacked polycrystalline anatase structure as observed. This is a typical feature of anodic TiO_2 nanotubes, i.e., they are not continuous tubes but an agglomerated form of anatase nanoparticles.

Figure 1e,f presents top-surface and cross-sectional SEM images of the final product after hydrothermal reactions with Pb acetate trihydrate (0.002 M) at 280 °C for 6 h. Rather unexpectedly, the product shows a uniform and densely packed nanowire array with a diameter of about 40 nm and a length of 10 μm. The nanowires are densely packed perpendicular to the Ti substrate, although topmost tips are slightly leaning.

(15) Prakasam, H. E.; Shankar, K.; Paulose, M.; Varghese, O. K.; Grimes, C. A. *J. Phys. Chem. C* **2007**, *111*, 7235.

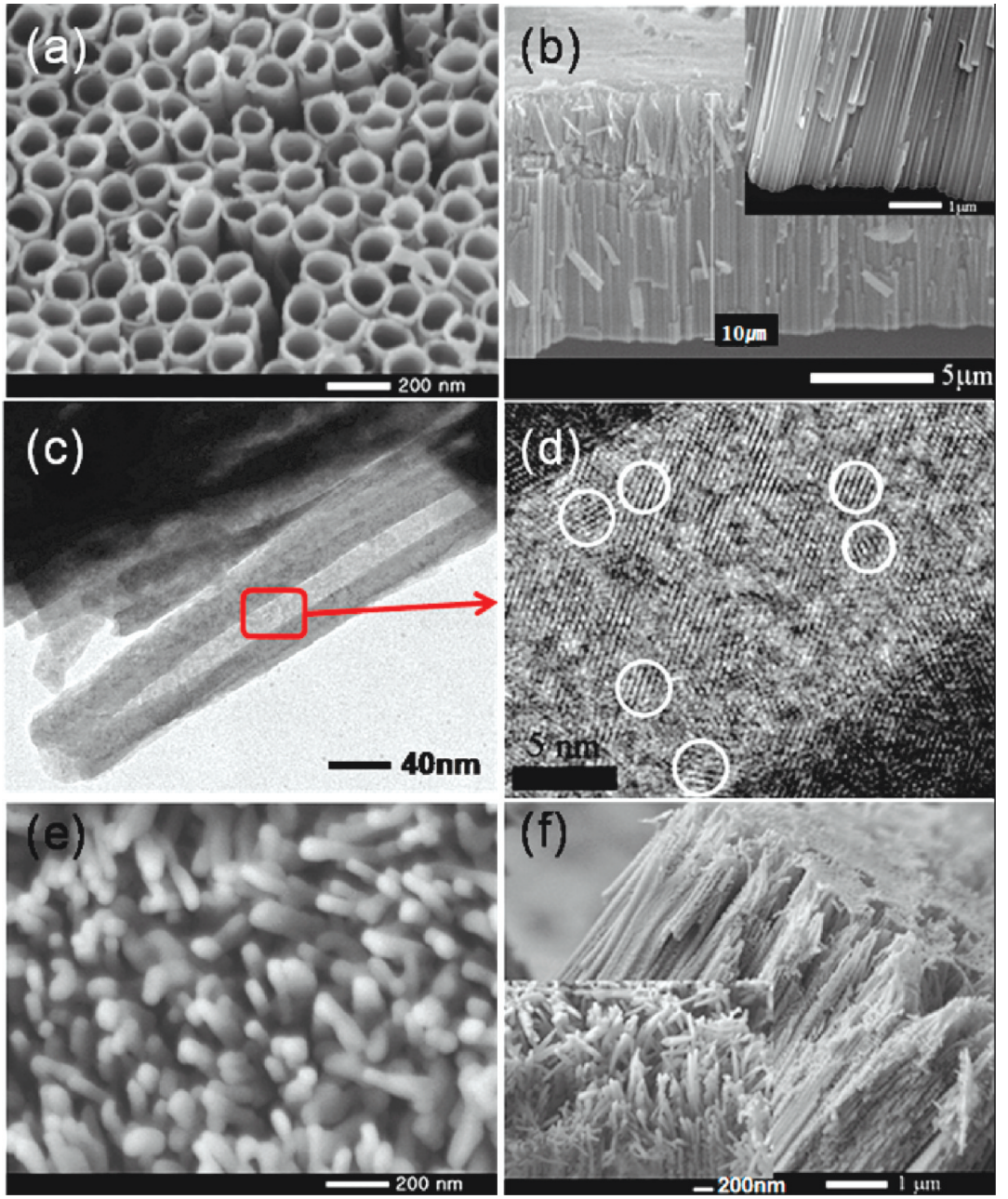

Figure 1. (a,b) FESEM images of anodized TiO_2 nanotubes. (c,d) TEM images of particle-stacked polycrystalline anatase TiO_2 nanotubes. (e,f) FESEM images of formed $PbTiO_3$nanowires.

Figure 2 shows a time series of the formation of $PbTiO_3$ nanowires by hydrothermal reaction of TiO_2 nanotubes. Figure 2b−d represents SEM images of the intermediate products taken out from the hydrothermal reactor in the middle of the reaction at 280 °C after 1.5 h, 3 h, and 4.5 h, respectively. These images of intermediates provide a critical clue to the mechanism of nanotube-to-nanowire transformation as discussed below.

Note that TiO_2 nanotubes, intermediate products, and $PbTiO_3$ nanowires all have the same length of 10 μm, but the diameter of nanowires (40 nm) is much smaller than the inner diameter of nanotubes (120 nm). It indicates that the nanowire originates from the tube not by filling its pores[16,17] but by some other process. The SEM images of intermediate products taken out from the hydrothermal reactor in the middle of the synthesis reaction (Figure 2b−d) show how nanotubes get swollen, are broken, and turn to wires. In the early stage of the hydrothermal reaction, the wall of nanotubes becomes thicker from 20 to 40 nm, making a tube diameter of 140 nm. This swelling of the wall could be understood by reaction of TiO_2 with Pb^{2+} to form $PbTiO_3$. At the same time, their shape is severely distorted and broken to become wires. It should be noted that the wall thickness of the distorted nanotubes (40 nm) is almost the same as the diameter of the nanowires. These images represent a

(16) Sun, X.; Li, Y. *Chem.—Eur. J.* **2003**, *9*, 2229.

(17) Yuan, Z. Y.; Su, B. L. *Colloid Surface A* **2004**, *241*, 173.

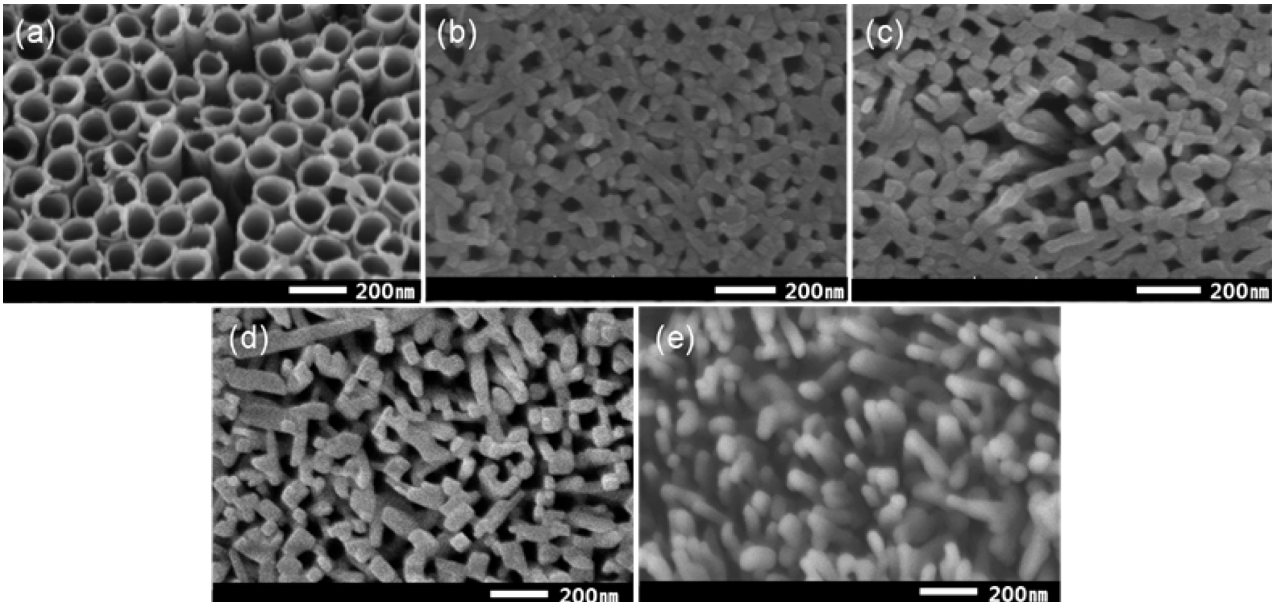

Figure 2. FESEM images of (a) anodized TiO_2 nanotubes prepared at 60 V for 30 min; (b, c, d, and e) $PbTiO_3$ intermediates obtained by hydrothermal treatment of anodized TiO_2 nanotubes at 280 °C for 1.5 h, 3 h, 4.5 h, and 6 h, respectively.

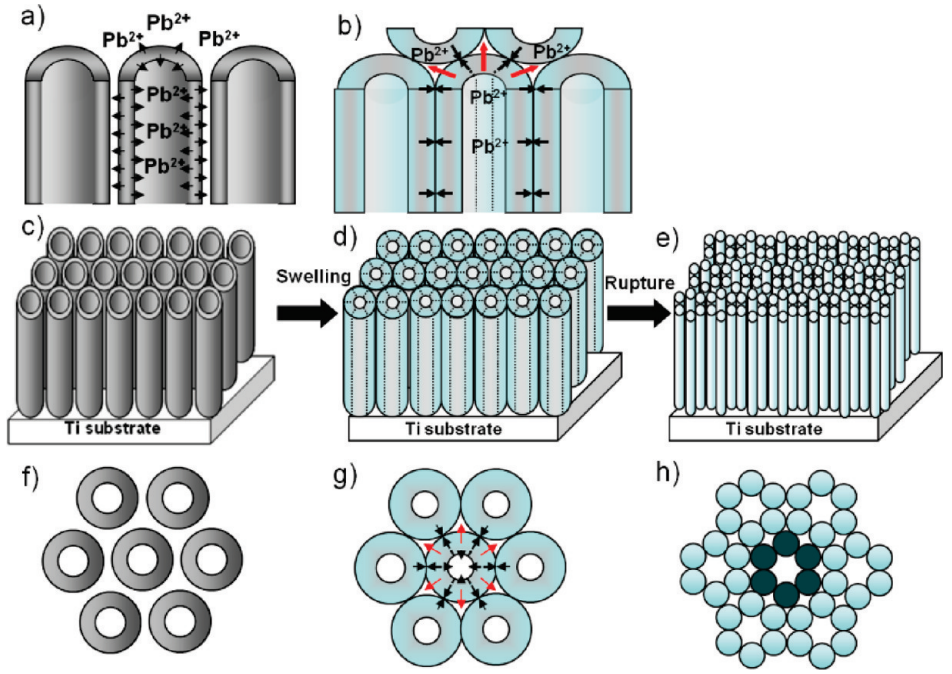

Figure 3. Formation mechanism of a perpendicular $PbTiO_3$ nanowire array on Ti substrate by hydrothermal treatment of anodized TiO_2 nanotubes: (a,c,f) anodized TiO_2 nanotubes on Ti foil at the initial state; (b,d,g) expanded nanotubes with friction planes during hydrothermal reaction at the intermediate state; (e,h) final $PbTiO_3$ nanowire product.

series of snap shots of the process of nanotube-to-nanowire transformation. From these observations, we can conclude that during the hydrothermal reaction of TiO_2 in Pb acetate solution, nanotubes become swollen and rupture to form nanowires, while TiO_2 changes to $PbTiO_3$.

On the basis of these observations, we propose a mechanism of $PbTiO_3$ nanowire fabrication via a TiO_2 nanotube. As shown in Figure 3a,b, when Pb ions enter TiO_2 nanotube walls, the wall thickness of the individual nanotube is expanded (swelling). When a tube swells (say, the center tube in Figure 3g), its wall collides with six neighboring tubes. The process generates expansion-force differences depending on whether it is directed to the contact point (black arrows) or empty space of the tubes (red arrows). This would form friction planes (dotted-line) between two expansion-forces directed into the empty space (red arrows) in Figure 3b,d,g. Then, 6-friction planes are formed in one tube, which lead to the rupture of an individual tube into 6 nanowires (Figure 3e,h). As a result of this swelling-and-rupture process, the TiO_2 nanotube array on the Ti substrate is transformed into the vertically aligned $PbTiO_3$ nanowire array as depicted in Figure 3c,d,e. In any case, by forming 6 nanowires from one tube, the density of nanowires becomes 0.228×10^{12} wires inch^{-2}

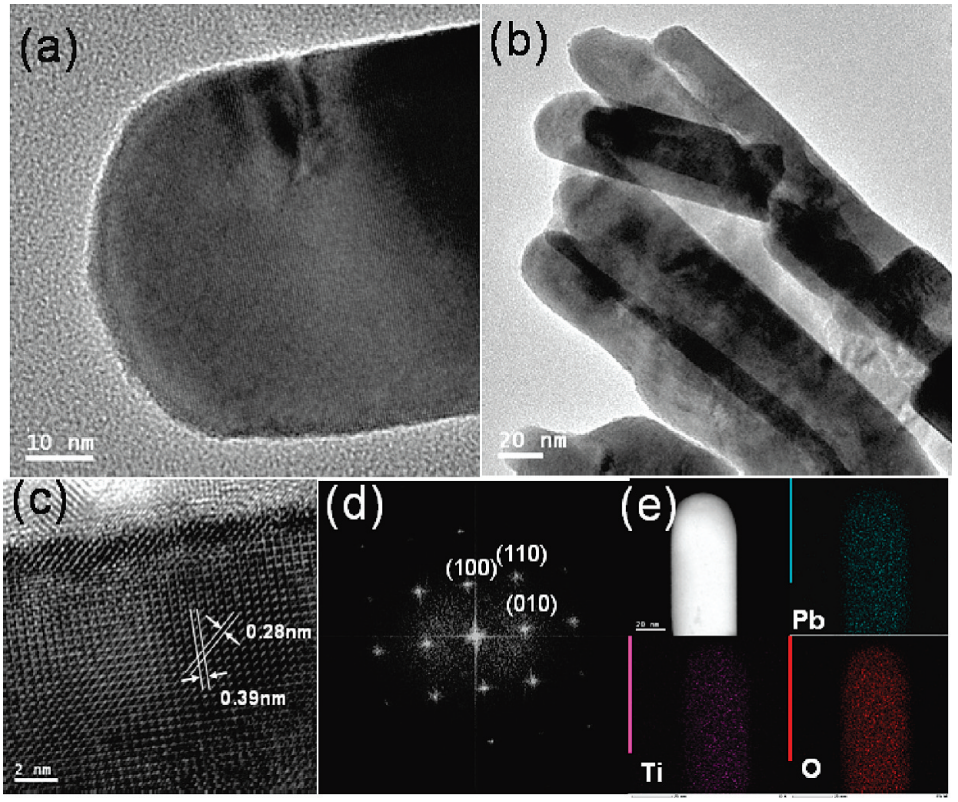

Figure 4. TEM images of the tips of the as-prepared $PbTiO_3$: single nanowire (a) and multiple nanowires (b). Representative high-resolution TEM (HRTEM) image (c), SAED pattern (d), and energy-dispersive X-ray spectroscopy (EDS) mapping (e) of the $PbTiO_3$ single nanowire.

corresponding to 0.228 Tb $inch^{-2}$ of ultrahigh density ferroelectric memory.

This force difference was operating because we started with the vertically aligned TiO_2 nanotube array of high density. Therefore, this synthesis method cannot be applied to randomly oriented nanotubes. Indeed, there are several previous reports that used anodic titanate nanotubes as the template to react with Pb salt in a hydrothermal reaction to obtain $PbTiO_3$.[13,14] But, only polycrystalline nanotubes were obtained in the previous works instead of single-crystalline nanowires as we presented here. The critical difference of our synthesis condition from that of previous works is the quality of TiO_2 nanotubes, the precursor to $PbTiO_3$ nanowires. Organic solvents such as ethylene glycol was used to achieve regular and uniform nanotubes as well as longer lengths relative to those of the products obtained in aqueous solution. Thus, only these high quality anodic titanate nanotubes would induce regular friction planes that make the nanotubes rupture regularly leading to the formation of uniform single crystal nanowires. Without these high quality nanotubes, the nanowire formation by the swelling-rupture mechanism is impossible, although the same hydrothermal reaction is employed.

3.2. Physical and Ferroelectrical Properties of the $PbTiO_3$ Nanowire Array. The nanowire array was further characterized to determine the structure. Figure 4a,b shows TEM images of the single and multiple of $PbTiO_3$ nanowires, and Figure 4c,d shows representative high resolution TEM images and selected area electron diffraction (SAED) patterns. The *d*-spacings estimated from the lattice fringes in Figure 4d are 0.39 and 0.28 nm, which correspond to (100) and (110) planes of $PbTiO_3$, respectively. The clean spot pattern of electron diffraction also indicates that the nanowire is a single crystal. The individual nanowire is composed of Pb, Ti, and O with the almost the same atomic ratio of Pb and Ti (Pb:Ti = 1:1) in the whole area as evident from EDS mapping (Figure 4e).

The unique characteristic of the proposed fabrication technique is the production of the single crystalline $PbTiO_3$ nanowires. It is important to confirm that the individual nanowire is entirely a single crystal of $PbTiO_3$. Figure 5 shows a series of TEM lattice fringe image of $PbTiO_3$ single nanowire obtained along the whole length of a single nanowire. As shown in Figure 5b-d, exactly the same lattice fringes are observed in the whole length of each nanowire without grain boundaries, defects, and dislocations, which indicate that the individual nanowire is single-crystalline. Thus, $PbTiO_3$ remains as particles in the nanotube state probably because of the curvature of the tubes, yet forms single crystals in nanowire state under hydrothermal conditions.

The X-ray diffraction (XRD) pattern in Figure 6a represents pure $PbTiO_3$ of the tetragonal phase (space group *P4mm*; **a** = 3.902 A; **c** = 4.158 A). Each reflection could be indexed according to JCPDS No. 78-0298. No other peaks are observed except for Ti peaks originated from the Ti substrate. However, our sample shows unusually strong (002) and (200) reflections, probably due to the aligned nanowire morphology. The tetragonal phase

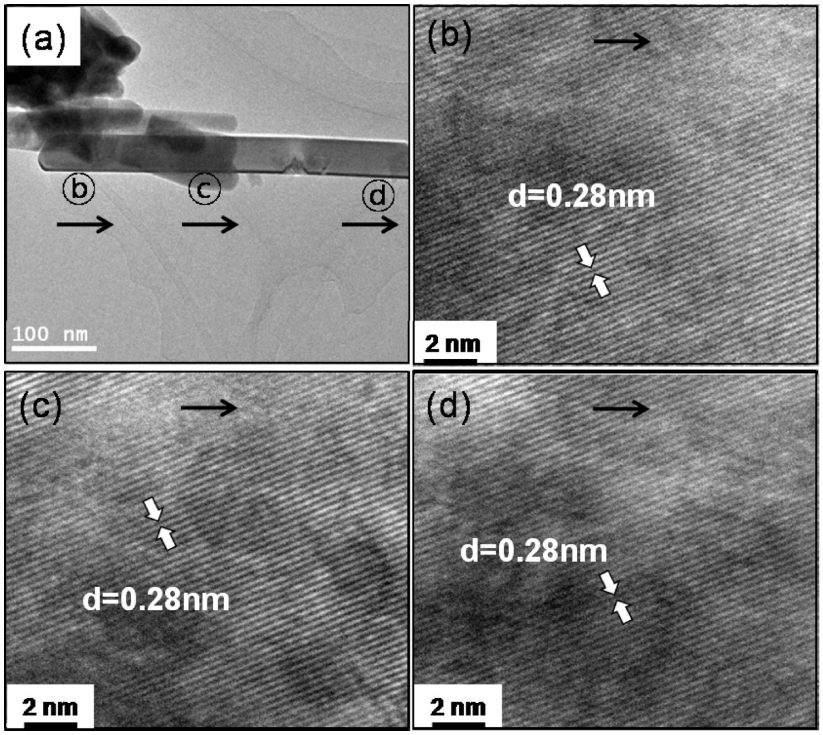

Figure 5. (a) TEM image of the as-prepared $PbTiO_3$ single nanowire and HRTEM images obtained at ⓑ, ⓒ, and ⓓ of the $PbTiO_3$ single nanowire in panel a. The *d*-spacing estimated from the lattice fringe is 0.28 nm, which corresponds to the (110) plane of $PbTiO_3$. The arrows show the direction of TEM observation.

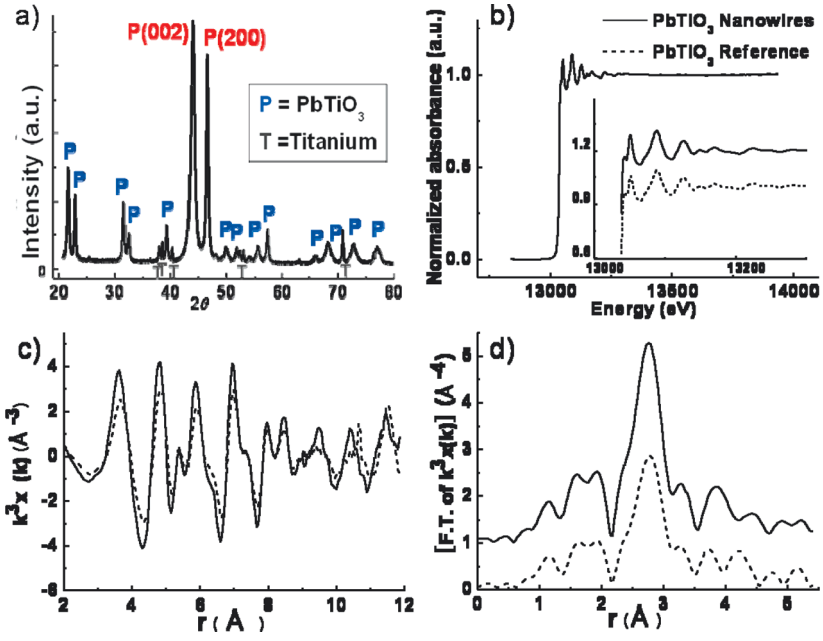

Figure 6. (a) XRD pattern of a $PbTiO_3$ nanowire array on Ti substrate. (b) X-ray absorption spectrum near the Pb-L_3 edge. The inset is magnified spectra (c) EXAFS oscillation $k^3x(k)$ functions and (d) their Fourier transforms of the as-prepared $PbTiO_3$ nanowire array film and reference $PbTiO_3$ (Aldrich).

of $PbTiO_3$ is known to have an excellent ferroelectric property.[18] Thus, the TiO_2 nanotube array grown on the Ti substrate has been transformed into a vertically aligned $PbTiO_3$ nanowire array on the Ti substrate by hydrothermal treatment. Extended X-ray absorption fine structure (EXAFS) was employed to study structure and local atomic arrangements of the $PbTiO_3$ nanowire array and reference $PbTiO_3$ (Aldrich). The EXAFS near the Pb-L_3 edge (Figure 6b) confirms the structural similarity of the prepared $PbTiO_3$ nanowire array to the reference $PbTiO_3$. The EXAFS oscillation k^3x functions and their Fourier transforms reveal that the as-prepared $PbTiO_3$ nanowire array has the same atomic distances including

(18) Ching-Prado, E.; Reynes-Figueroa, A.; Katiyar, R. S.; Majumder, S. B.; Agrawal, D. C. *J. Appl. Phys.* **1995**, *78*(3), 1920.

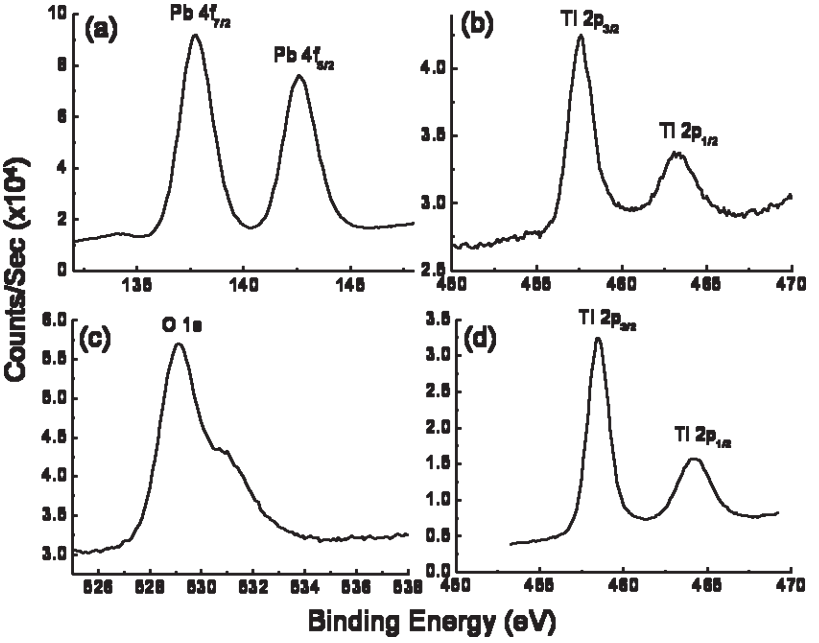

Figure 7. Narrow scan XPS spectrum of the (a) Pb 4f peak, (b) Ti 2p peak, and (c) O 1s peak in the $PbTiO_3$ nanowire array film, and (d) Ti 2p peak in anodic TiO_2 nanotubes.

three Pb−O pairs and two Pb−Ti pairs as those of reference $PbTiO_3$.[19−21]

Figure 7 shows the XPS spectra for Pb 4f, Ti 2p, and O 1s of the $PbTiO_3$ nanowire array film and Ti 2p of the TiO_2 nanotubes film. Figure 7a shows two valence states, the Pb $4f_{7/2}$ and Pb $4f_{5/2}$ peaks. The binding energy of symmetric and narrow Pb $4f_{7/2}$ peak is 137.8 eV, which is in agreement with the literature.[22] There is a difference of the binding energies between Ti $2p_{3/2}$ peaks of the $PbTiO_3$ nanowire (457.6 eV) and the TiO_2 nanotube (458.5 eV) (Figure 7b and d). This shift to a smaller binding energy of the Ti $2p_{3/2}$ peak is related to the increase in the polarizability of the cation when TiO_2 converts into $PbTiO_3$.[23] The main peak (Figure 7c) at low binding energy of the O 1s XPS spectra indicates the oxygen in the lead titanate thin film, and the shoulder at higher binding energy represents the presence of the hydroxyl group or oxygen contaminants on the surface of the sample, which is a very common feature in this kind of thin film sample. These interfacial characteristics are important to determine the electrical behavior reliability in integrated devices.[24,25]

The individual $PbTiO_3$ nanowire in the vertical array has a tetragonal phase and single crystalline structure. These $PbTiO_3$ nanomaterials generally have superior ferroelectric properties relative to those of bulk materials. If the as-prepared individual lead titanate nanowire has ferroelectric properties, then it is expected to have an improved efficiency than the thin film when it is applied in electronic devices because of rapid vectorial electron and thermal transport and better memory capacity. The well-aligned ferroelectric nanowire arrays on a substrate are also suitable for three-dimensional device elements in miniaturized ferroelectric devices.

Thus, the ferroelectric properties were investigated by piezo-response force microscopy (PFM). Figure 8 shows the same scale SEM image, topography, vertical polarization phase, and amplitude images. Figure 8b-d was simultaneously obtained by PFM for the same area of the sample. Topography in Figure 8b is consistent with the SEM image and shows the positions of nanowires. In Figure 8c, the bright area represents upward polarization, and the dark area denotes the downward polarization. It also shows the boundaries of domains with different directions. The amplitude of vertical polarization is quite strong as shown in Figure 8d. Therefore, Figure 8c,d shows definite phase change and high amplitude of vertical polarization, respectively. Thus, the ferroelectric property is observed over the whole area of the nanowire arrays. We also determined the local piezoelectric property of a single nanowire (marked with an arrow in Figures 8b-d) depending on the applied voltage. The well-defined, characteristic butterfly loop of the piezoelectric coefficient magnitude in Figure 8e indicates a good piezoelectric behavior, and the switching phase diagram in Figure 8f reveals the direction of spontaneous polarization. This piezoelectric hysteresis loop proves the excellent ferroelectricity of the individual nanowire.[14,26,27]

(19) Terauchi, H.; Iida, S.; Tanabe, K.; Maeda, H.; Hida, M.; Kamijo, N.; Takashige, M.; Nakamura, T. *J. Phys. Soc. Jpn.* **1984**, *53*(5), 1598.
(20) Feth, M. P.; Weber, A.; Merkle, R.; Reinohl, U.; Bertagnolli, H. *J. Sol-Gel Sci. Technol.* **2003**, *27*, 193.
(21) Miyanaga, T.; Diop, D.; Ikeda, S. I.; Kon, H. *Ferroelectrics* **2002**, *274*, 41.
(22) Pederson, L. R. *J. Electron Spectrosc. Relat. Phenom.* **1982**, *28*, 203.
(23) Murata, M.; Wakino, K. *J. Electron Spectrosc. Relat. Phenom.* **1975**, *6*, 459.
(24) Lu, C. J.; Kuang, A. X.; Huang, G. A. *J. Appl. Phys. Chem.* **1996**, *80* (1), 202.
(25) Bao, D.; Wu, X.; Zhang, L.; Yao, X. *Thin Solid Films* **1999**, *350*, 30.
(26) Poyato, R.; Huey, B. D.; Padture, N. P. *J. Mater. Res.* **2006**, *21*(3), 547.
(27) Lee., S. H.; Yang., C. H.; Jeong., Y. H.; Birge., N. O. *Phys. B* **2006**, *383*, 31.

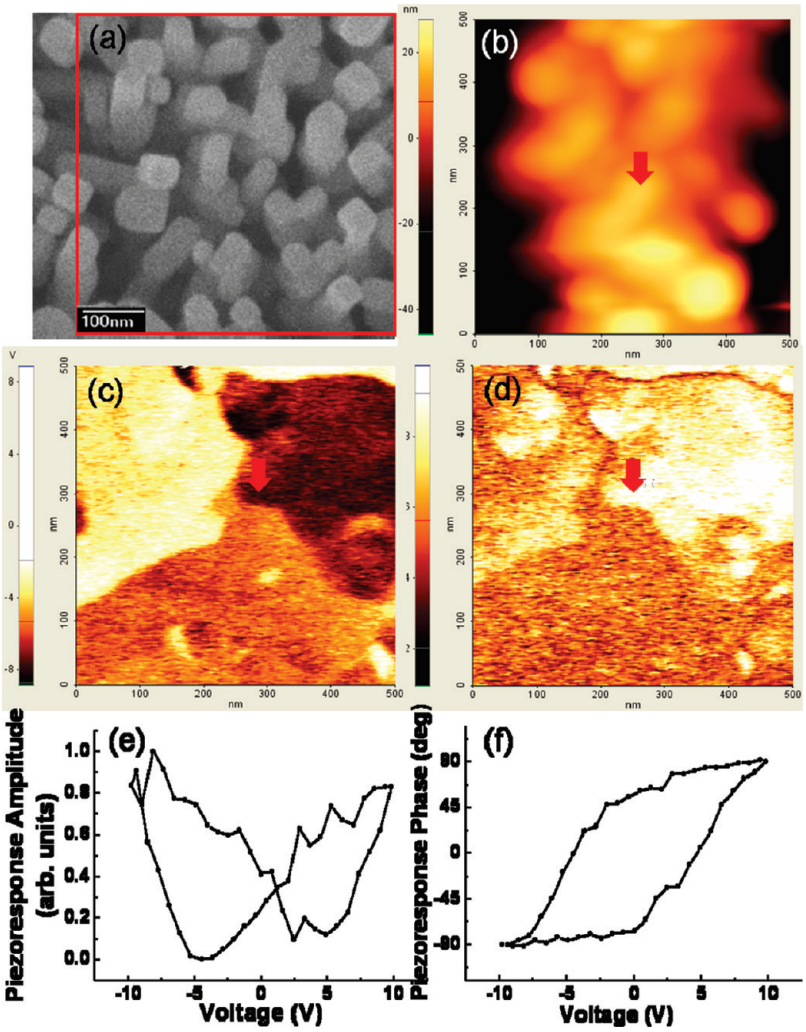

Figure 8. Images of the as-synthesized $PbTiO_3$ nanowire array: (a) SEM image of the same magnification as that for b−d; (b) topography, (c) vertical polarization phase, and (d) vertical polarization amplitude from PFM. Images in b, c, and d are simultaneously obtained by PFM for the same area of the sample. Piezoelectric hysteresis loop measured at the marked point in b, c, and d on a single $PbTiO_3$ nanowire: (e) piezoresponse amplitude and (f) piezoresponse phase diagram.

4. Conclusions

In this study, we fabricated a vertically well-aligned tetragonal-phase $PbTiO_3$ nanowire array grown on Ti substrate from a hydrothermal reaction of anodic anatase TiO_2. We described the swelling-and-rupture mechanism for nanowire formation, in which individually well-developed nanotubes are swollen and broken along the friction planes because of differences in the directions of the expansion force. The lead titanate nanowire has a single crystalline structure, appropriate atomic composition, and tetragonal phase $PbTiO_3$. The unique synthesis method reported here to obtain the vertically aligned $PbTiO_3$ nanowire array film is based on simple low-temperature solution processing. We can easily control the length and diameter of the nanowires as needed by controlling the size and wall thickness of nanotubes by adjusting anodization conditions. Furthermore, it is expected that the other titanate-based perovskite materials can be synthesized by this method.

Acknowledgment. This work was supported by Korea Center for Artificial Photosynthesis (KCAP) and Brain Korea 21 program funded by the Ministry of Education, Science, and Technology of Korea.